J. Kor. Soc. Cloth. Ind.
Vol. 2, No. 5, pp.443-449(2000)
<Transaction>

Analysis of the Relative Velocity of Friction Surface in Cone Drum False Twisting Mechanism

Choon Gil Lee

Dept. of Textile and Fashion Technology, Kyungil University, Kyungsan, Korea

Abstract : An investigation of the relative velocity of friction surface for the newly developed cone drum twister texturing mechanism is reported. The cone drum twister is one of the outer surface contacting friction-twisting devices in false-twist texturing. In this cone drum twister, a filament yarn passes over the surface of the cone drum that rotates by passing the yarn without a special driving device. This research is theoretically composed of the analysis of the false twisting mechanism. The equations were derived by using the conical angle of the cone drum, projected wrapping angle, and yarn helix angle. Theoretical values of the relative velocity of friction surface were calculated and discussed. It is shown that, as the projected wrapping angle increased, the relative velocity of friction surface decreased. But as the conical angle increased the relative velocity of friction surface also increased.

Key words : relative velocity of friction surface, cone drum twister, outer surface contacting friction-twisting device, conical angle, projected wrapping angle

NOMENCLATURE

- A Length of oo' (mm)
- B Length of bo' (mm)
- b Beginning point of false twist inserting region
- c End point of false twist inserting region
- D Velocity of friction surface (mm/sec)
- D_b Velocity of friction surface at point b (mm/sec)
- D_c Velocity of friction surface at point c (mm/sec)
- $\bar{e}$ Mean length of filaments in the length h of twisted yarn (mm)
- h Length of one turn of twist (mm)
- l Length of filament yarn in twisting zone, bc (mm)
- l_o Length of bc in the flat drum (mm)
- n Number of filaments crossing unit area perpendicular to the filament axis
- p Any point on the line bc
- R Radius of the filament yarn (mm)
- r Cone drum radius at any point (mm)
- r_b Cone drum radius at point b (mm)
- r_c Cone drum radius at point c (mm)
- s Length of bp (mm)
- α Angle between ob and op in the opening out diagram
- α_c Conical angle of cone drum
- α_o Angle between ob and oc in the opening out diagram
- β Angle between the yarn axis and the cone drum axis
- θ Surface helix angle of the filament yarn in twisting zone
- ξ Angle of wrap (bp region) on the friction surface as seen perpendicular to the yz plane
- ξ^* Angle of wrap (bc region) on the friction surface as seen perpendicular to the yz plane
- ϕ Angle between the filament yarn axis and the direction of friction surface movement
- ω Angular velocity of cone drum (rad/sec)

Corresponding author; Choon Gil Lee
Tel. +82-53-850-7203, Fax. +82-53-850-7605
E-mail: cglee@bear.kyungil.ac.kr

INTRODUCTON

The false twist methods have been used in synthetic fiber industry for the filament yarn texturing process. All kinds of conventional false twist methods have the drive systems for inserting twist to the filament yarns. But the cone drum twister has no drive system for inserting false twist. A filament yarn passes over the surface of the cone drum which rotates by the passing yarn without a special driving device.

The effects of heater temperature, linear density, draw ratio, projected wrapping angle, and conical angle on the false twisting tension and the yarn helix angle of the texturing yarns in the cone drum twister and the effects of heater temperature, linear density, draw ratio, and pro-

jected wrapping angle on the tenacity, crimp rigidity, skein shrinkage, breaking elongation of textured yarn produced by the cone drum twister were studied experimentally in previous studies (Lee and Kang, 1996). And the effects of stud radius on dimensionless torque and physical properties of the textured yarns in the stud type cone drum twister also had been studied (Lee, 1995). It showed that stud radius was a very important factor in the stud type cone drum texturing device.

The purpose of this paper is to develop theoretical relations between cone drum geometry and yarn geometry, especially to calculate the relative velocity of friction surface of the system. The relative velocity of friction surface of the cone drum twister is used to calculate drag angle, tension and torque of the yarns using in this apparatus.

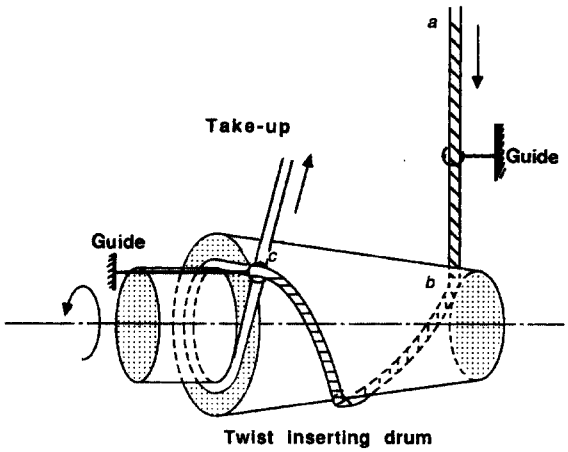

Fig. 1. Schematic diagram of the cone drum type draw texturing machine.

THEORETICAL ANALYSIS

The schematic diagram of the cone drum type draw texturing machine is shown in Fig. 1. This texturing process consists of a pair of feed rollers, a heater for setting deformed yarn, a pair of cone drum twisters which force yarn to rotate, and a pair of take-up rollers. Fig. 1 illustrates the principle of the twist inserting mechanism by the cone drums. The false twist is inserted on the twisting region by friction between the filament yarn and the rotating cone drum surface. Therefore, the cone drum twister is one of the outer surface contacting friction-twisting devices in false-twist texturing. In this cone drum twister, a filament yarn passes over the surface of the cone drum which is rotated by the passing yarn which is wrapped around the cone drum stud without a special driving device.

Theoretically in order to analyze the relative velocity of friction surface of the cone drum twister, the false twisting contact region was considered. Our treatment of the theoretical analysis of cone drum twister texturing process incorporates several simplifications and assumptions in order to obtain a reasonably uncomplicated analysis. In the analysis given below, it is assumed that:

(1) The filament yarn path remains straight in the open out diagram of the false twisting contact region, i.e., the yarn lies on the shortest path in the false twisting contact region.

(2) The angle of the false twist in the false twisting contact region is constant.

(3) The yarn is in continuous contact with the friction surface of the cone drum.

(4) The normal forces between the filament yarn and cone drum in the false twisting contact region are constant.

(5) The yarn maintains a circular cross-section, radius R

Length of false twisting contact region

In Fig. 2 we see that length of $\overline{ob}$ and length of $\overline{oc}$ are

$$\overline{ob}=x_c\sec\frac{\alpha_c}{2}=r_b\operatorname{cosec}\frac{\alpha_c}{2} \tag{1}$$

and

$$\overline{oc}=x_c\sec\frac{\alpha_c}{2}=r_c\operatorname{cosec}\frac{\alpha_c}{2}. \tag{2}$$

And in Fig. 2(b) we see that

$$\overline{ob}\cdot\ \alpha = r_b\cdot\ \xi^* \tag{3}$$

and

$$\overline{oc}\cdot\ \alpha_0 = r_c\cdot\ \xi^*. \tag{4}$$

From the above two Equations we find that

$$\alpha_0=\frac{r_b\cdot\xi^*}{\overline{ob}}\left(=\frac{r_c\cdot\xi^*}{\overline{oc}}\right). \tag{5}$$

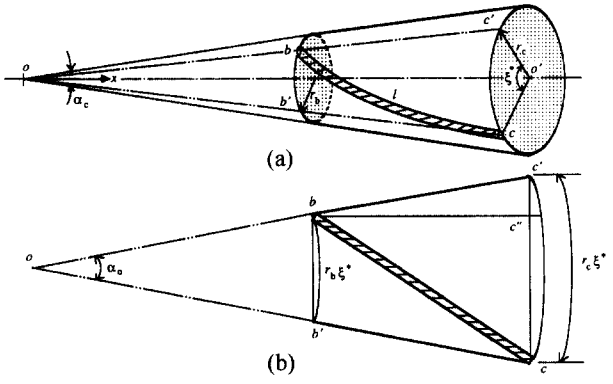

Fig. 2. Opening out diagram of the friction surface.

By inserting Equation (1) or Equation (2) into Equation (5) and simplifying we get

$$\alpha_o = \xi^* \sin\frac{\alpha_c}{2}. \tag{6}$$

Using this Equation we can derive the equation for the length of false contacting region, l.

In Fig. 2(b) we see that $\angle c'bc=\alpha_o/2$. Therefore the following relations are given from the open out diagram of the friction surface :

$$\overline{bc}''=(\overline{bc}-\overline{ob})\cos\frac{\alpha_0}{2}, \tag{7}$$

$$\overline{bb}'=2\overline{ob}\sin\frac{\alpha_0}{2}, \tag{8}$$

and $$\overline{cc}'=2\overline{oc}\sin\frac{\alpha_0}{2}. \tag{9}$$

And we can also derive the length of the false contacting region easily as follows :

$$l=\overline{bc}=\left\{\left(\overline{bb}'+\frac{\overline{cc}'+\overline{bb}'}{2}\right)^2+(\overline{bc}'')^2\right\}^{\frac{1}{2}} \tag{10}$$

By inserting Equations (7), (8) and (9) into the above Equation, we get

$$l=\left\{(\overline{oc}-\overline{ob})^2\cos^2\frac{\alpha_0}{2}+(\overline{ob}+\overline{oc})^2\sin^2\frac{\alpha_0}{2}\right\}^{\frac{1}{2}}. \tag{11}$$

By using Equations (1), (2) and (6), the equation for the length of the false contacting region, l is given as follows :

$$l=\left[\left\{\operatorname{cosec}\frac{\alpha_c}{2}(r_c-r_b)\right\}^2\cos^2\left(\frac{\xi^*}{2}\sin\frac{\alpha_c}{2}\right)+\left\{\operatorname{cosec}\frac{\alpha_c}{2}(r_b+r_c)\right\}^2\sin^2\left(\frac{\xi^*}{2}\sin\frac{\alpha_c}{2}\right)\right]^{\frac{1}{2}} \tag{12}$$

given that $x_c=x_b+40$ mm and $r_b=6$ mm, we have

$$r_c=\left(r_b\cot\frac{\alpha_c}{2}+40\right)\tan\frac{\alpha_c}{2}. \tag{13}$$

Fig. 3 shows that the relationship between the conical angle and relative yarn contact length at various projected wrapping angles. Through this figure we can see that the relative yarn contact length increases as the conical angle and projected wrapping angle increase.

Change of forward velocity of the filament yarn by the change of twist angle

Let the length of the filaments in the length h of twisted yarn be e, the number of filaments crossing the unit area perpendicular to the filament axis be n, and the false twist

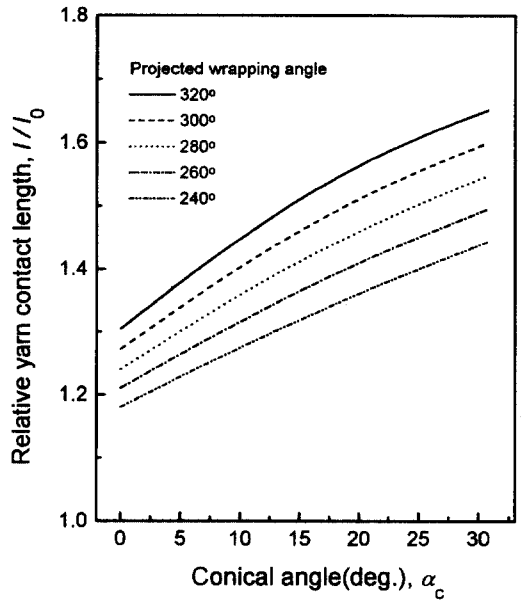

Fig. 3. Plots of the relative yarn contact length verses the conical angle at various projected wrapping angles.

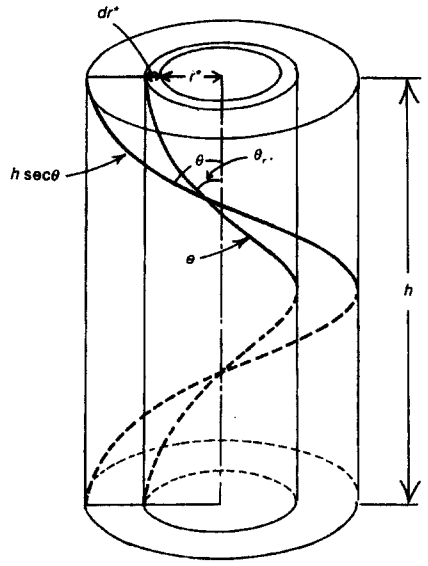

Fig. 4. Idealized helical yarn geometry.

angle at the radius of r be θ_{r^*} in Fig. 4. Then we can see that

$$dn = n \cdot 2\pi r^* \, dr^* \cdot \cos\theta_r^*. \tag{14}$$

In the idealized helical yarn structure, from Equation (14), we get

$$dn=\frac{nh}{2\pi}dl. \tag{15}$$

Let the forward velocity of the filament yarn in the false twisting region be V_1, the time taken moving length

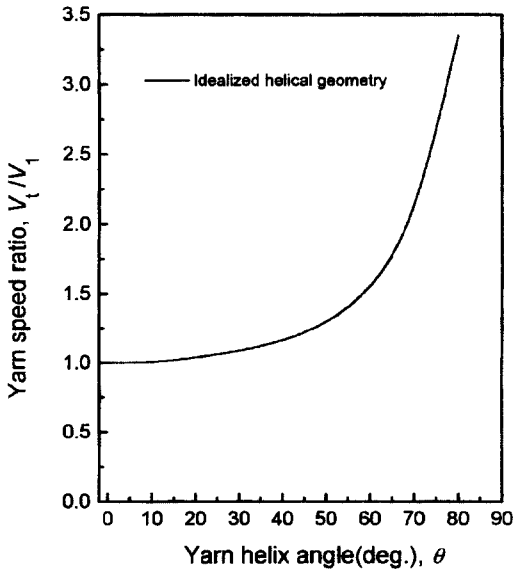

Fig. 5. Effect of yarn helix angle on the yarn speed ratio.

h be t, and the delivery velocity of the filament yarn be V_t then we see that

$$V_t=\frac{e}{t} \tag{16}$$

and

$$V_1=\frac{h}{t} \tag{17}$$

Therefore, if we let the helix angle of the yarn surface be θ we get

$$V_t=\frac{1}{t}\cdot\frac{\int_h^{h\sec\theta} e\,dn}{\int_h^{h\sec\theta_b} dn}. \tag{18}$$

By inserting Equations (15) and (18) into Equation (17) and simplifying we get

$$V_1=\frac{2V_t}{1+\sec\theta}. \tag{19}$$

Fig. 5 shows the effect of the yarn helix angle on the yarn speed. Through this result we can understand that the yarn helix angle in the twisting region highly affects the yarn speed over the twist inserting zone.

Velocity of friction surface

Fig. 6 illustrates the rotating cone drum at a constant angular velocity and the velocity diagram over the friction surface. Given that the radius of the stud is 4 mm in Fig. 1, the angular velocity of the cone drum is given by

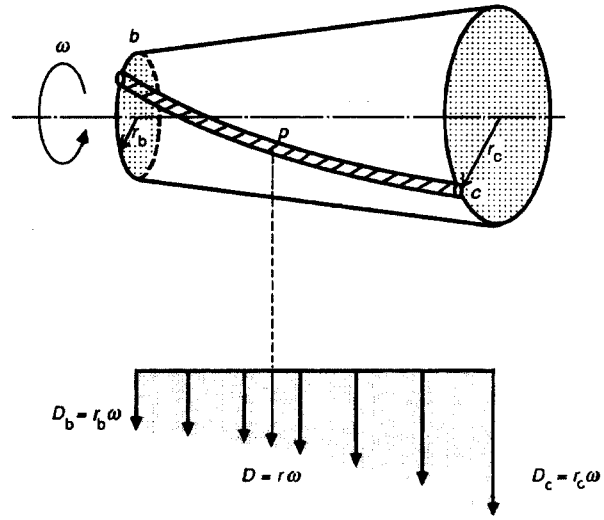

Fig. 6. Velocity of friction surface.

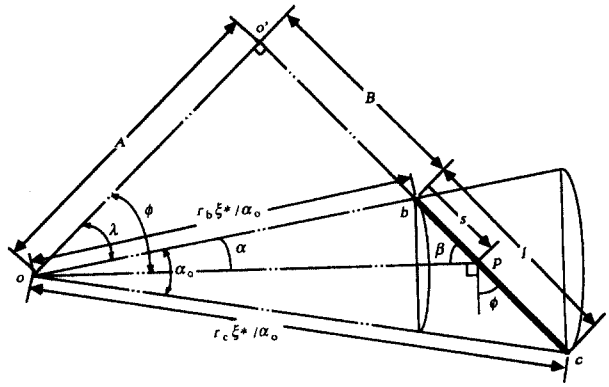

Fig. 7. Relationship between the cone drum radius at any point and the length between the beginning point b and any point p on the false twisting region.

$$\omega=\frac{V_t}{4} \tag{20}$$

and in Fig. 7 we see that

$$\overline{op}^2=A^2+(B+s)^2 \tag{21}$$

and

$$\overline{op}=\frac{\xi^*}{\alpha_o}r \tag{22}$$

where s is the length between the beginning point b and any point p on the false twisting region, A is the length of oo', and B is the length of bo'.

Therefore from Equations (21) and (22) we obtain that

$$\frac{\xi^*}{\alpha_o}r=\sqrt{A^2+(B+s)^2} \tag{23}$$

and at point b and c;

$$\overline{ob}=\frac{\xi^*}{\alpha_o}r_c=\sqrt{A^2+B^2} \tag{24}$$

and

$$\overline{oc}=\frac{\xi^*}{\alpha_o}=\sqrt{A^2+(B+l)^2}. \tag{25}$$

From Equations (24) and (25) it follows that

$$B=\frac{1}{2l}\left\{\left(\frac{\xi^*}{\alpha_o}\right)^2(r_c^2-r_b^2)-l^2\right\} \tag{26}$$

and by inserting the above equation into Equation (24) and simplifying we obtain

$$A=\left[\left(\frac{\xi^*}{\alpha_o}r_b\right)^2-\frac{1}{4l^2}\left\{\left(\frac{\xi^*}{\alpha_o}\right)(r_c^2-r_b^2)-l^2\right\}^2\right]^{\frac{1}{2}}. \tag{27}$$

By inserting Equations (26) and (27) into Equation (23) and simplifying with respect to r we obtain

$$r=\left[r_b^2+\frac{1}{l}\left\{r_c^2-r_b^2-\left(\frac{\alpha_o l}{\xi^*}\right)^2\right\}s+\left(\frac{\alpha_o}{\xi^*}\right)^2 s^2\right]^{\frac{1}{2}}. \tag{28}$$

The velocity of friction surface D is obtained as a function of s by inserting Equations (6) and (20) into the above Equation and simplifying;

$$D=r\omega=\frac{V_f}{r_d}\left[r_c^2+\frac{1}{l}\left\{r_c^2-r_b^2-\left(\sin^2\frac{\alpha_c}{2}\right)l^2\right\}\right]^{\frac{1}{2}}. \tag{29}$$

RESULTS AND DISCUSSION

Plotting of the relative velocity of friction surface of the cone drum twister

Fig. 8 shows the plots of relative velocity of the friction surface verses the length of the contact region from the beginning point of the false twist inserting region to any point on the line of the false twist inserting region at various conical angles under the projected wrapping angle of 240°. Through this figure we see that the relative velocity of the friction surface increases as the length of the contact region from the beginning point of the false twist inserting region to any point on the line of the false twist inserting region increases.

In Fig. 9 the tendency of increasing relative velocity is similar as that of in Fig. 8. Fig. 9 was plotted under the projected wrapping angle of 320°. The increasing rate of relative velocity in Fig. 9 is lower than that of in Fig. 8.

Fig. 10 shows plots of the relative velocity of friction surface verses length of the contact region from the beginning point of the false twist inserting region to any point on the line of the false twist inserting region at various projected wrapping angles under the conical angle of 10°. This figure shows that the relative velocity of friction surface increases the same as the previous figures. Fig. 11 is the plot of relative velocity of friction surface under the conical angle of 30.75°.

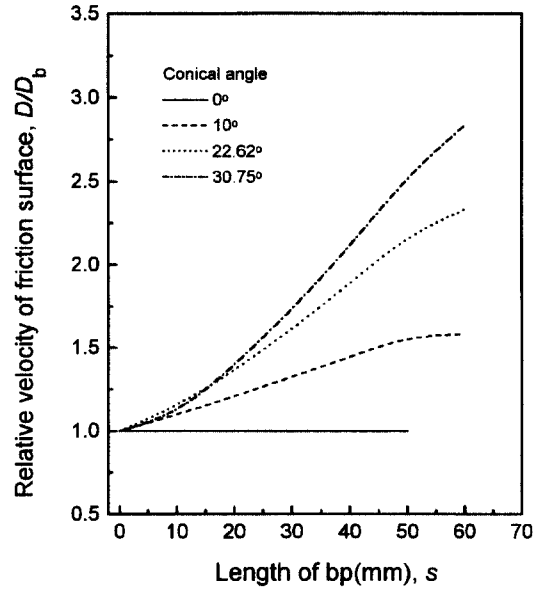

Fig. 8. Plots of the relative velocity of friction surface verses length $\overline{bp}$ at various conical angles under the projected wrapping angle of 240°.

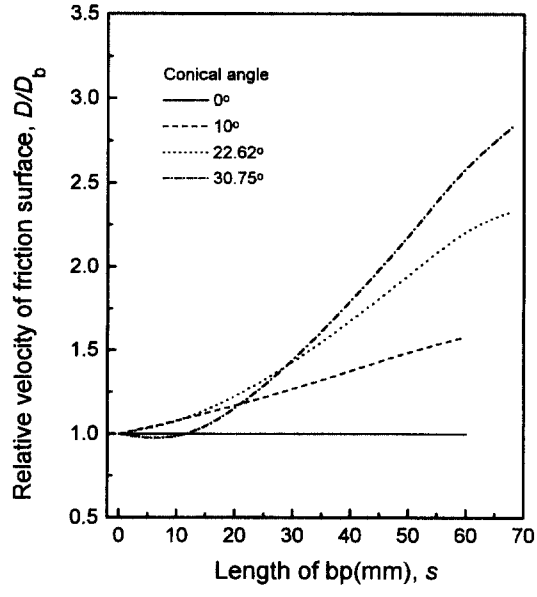

Fig. 9. Plots of the relative velocity of friction surface verses length $\overline{bp}$ at various conical angles under the projected wrapping angle of 320°.

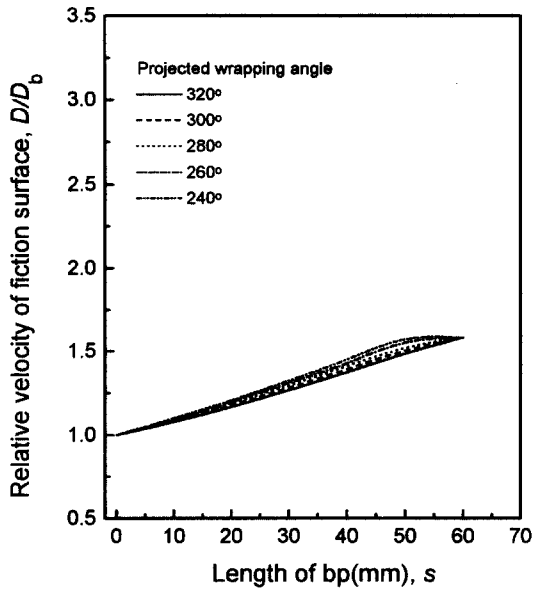

Fig. 10. Plots of the relative velocity of friction surface verses length $\overline{bp}$ at various projected wrapping angles under the conical angle of 10°.

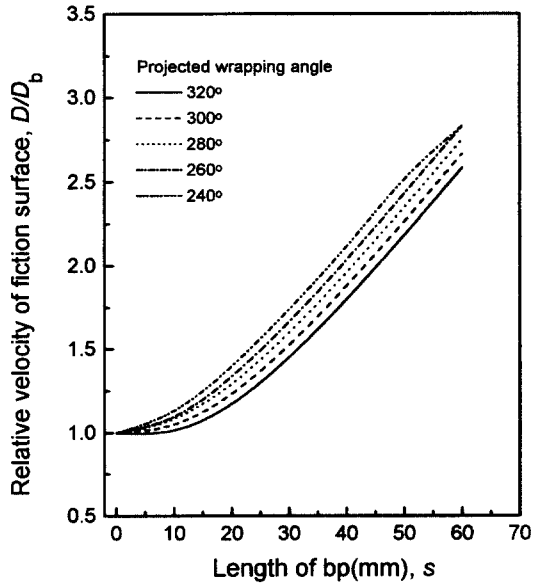

Fig. 11. Plots of the relative velocity of friction surface verses length $\overline{bp}$ at various projected wrapping angles under the conical angle of 30.75°.

Effect of the conical angle on the relative velocity of friction surface

Figs. 8 and 9 show the effect of the conical angle of the cone drum on the relative velocity of friction surface. In the flat drum, i.e., the conical angle of 0 degree, the relative velocity is constant because of the constant velocity of friction surface over the twist inserting zone. But as the conical angle increases the increasing rate of relative velocity also increases. It is necessary that the relative velocity for inserting twists are more effective to develop higher dimensionless torque for various filament yarn, hence the conical angle plays an important role in inserting false twists because the conical angle greatly affects relative velocity.

Effect of the projected wrapping angle of false twisting zone on the relative velocity of friction surface

Figs. 10 and 11 show the increase of the relative velocity of friction surface at various projected wrapping angles according to the increase of the contacting length from the beginning point to any point on the line of false twist inserting region. These figures show that the relative velocity of friction surface increases the same as previous figures, but the higher the projected wrapping angle, the lower the relative velocity of friction surface. The difference of the relative velocity between the projected wrapping angles under the conical angle of 30.75° is higher than that of the relative velocity between projected wrapping angles under the conical angle of 10°.

CONCLUSIONS

Newly developed cone drum twister texturing mechanism was investigated theoretically. The cone drum twister can be classified as one of the outer surface contacting friction-twisting devices in false-twist texturing. The equations were derived by using the conical angle of cone drum, wrapping angle, and cone drum radius. Through the calculation of theoretical values of the relative velocity of friction surface the following results were obtained.

1. The relative velocity of friction surface increases as the length of contacting region from the beginning point to any point on the line of the false twist inserting region increases.
2. In flat drum, i.e., the conical angle of 0 degree, the relative velocity is constant because of the constant velocity of friction surface over the twist inserting zone.
3. As the conical angle increased the increasing rate of relative velocity also increased.
4. The higher the projected wrapping angle the lower the relative velocity of the friction surface.
5. Difference of the relative velocity between projected wrapping angles under the conical angle of 30.75° is higher than that of the relative velocity between the projected wrapping angles under the conical angle of 10°.

REFERENCES

Lee C. G. and Kang T. J. (1996) False twist tension and false twist angle in the cone drum twister. *Journal of Korean Fiber Society*, **33**(3), 248-256.

Lee C. G. and Kang T. J. (1996) On the physical properties of textured yarn produced by the cone drum twister. *Journal of Korean Fiber Society*, **33**(5), 393-402.

Lee C. G. (1995) Studies on the development of a stud type cone drum twister (I). *Journal of Korean Fiber Society*, **32**(7), 621-634.

Greenwood K. (1975) The present situation and future prospects of the false-twist process. *J. Textile Inst.*, **12**, 420-425.

Arthur D. F. and Weller A. F. (1959) The principles of friction twisting. *J. Textile Inst.*, T66-T72.

Morris W. J. and Denton M. J. (1975) An improved method of friction twising in the false-twist-texturing process (Part II) Thoretical relations between yarn and processing parameters in the improved friction spidle. *J. Textile Inst.*, **3**, 123-128.

Howell H. G. (1953) The general case of friction of a string round a cylinder. *J. Textile Inst.*, T359-362.

Morton W. E. and Permanyer F. (1948) Torque-twist relations in single and multiple rayon filaments. *J. Textile Inst.*, T371-T380.

Greenwod K. and Grigg P. J. (1985) The development of twist in a false-twist texturing machine eith a friction twister. *J. Textile Inst.*, **4**, 244-263.

Theaites J. J. (1984) The mechanics of friction-twisting reassessed (Part I) The yarn path in a disc spindle. *J. Textile Inst.*, **4**, 285-297.

Denton M. J. (1975) The structural geometry and mechanics of false-textured yarns. *J. Textile Inst.*, **2**, 80-86.

Thwaites J. J. (1985) The mechanics of friction-twisting reassessed (Part II) Tension and torque generation in the disc spindle. *J. Textile Inst.*, **3**, 157-170.

Thwaites J. J. (1976) Mechanics of texturing thermoplastic yarns (Part IV) The origin and significance of the torsional behavior of the false-twist threadline. *Text. Res. J.*, **46**, 886-892.

Denton M. J. (1975) Tension ratio and slip in friction-twisting. *J. Textile Inst.*, **8**, 303-306.

Thwaites J. J. (1978). The dynamics of the false-twist process (Part II) A theoretical model. *J. Textile Inst.*, **9**, 276-286.

Thwaites J. J. Hooper, C. W. (1981). The dynamics of the false-twist process (Part III) Experiments with fully drawn yarn. *J. Textile Inst.*, **6**, 239-248.

Hearle J. W. S. (1979) Studies in friction-twisting (Part I) A simple treatment of the slipping mode. *J. Textile Inst.*, **7**, 287-297.

Hearle J. W. S. Beech, S. R. (1980) Studies in friction-twisting (Part II) The positive mode. *J. Textile Inst.*, **5**, 225-235.

(Received December 19, 2000)